Proceedings of the Canadian Society for Mechanical Engineering International Congress
32nd Annual Conference of the Computational Fluid Dynamics Society of Canada
Canadian Society of Rheology Symposium
CSME-CFDSC-CSR 2025
May 25–28, 2025, Montréal, Québec, Canada

Effect of Raster Angle on the Anisotropic Behavior of 3D-Printed TPU Under Uniaxial and Planar Loading Conditions

Ragab Etiwa[1], Aleksander Czekanski[1*]
[1]Department of Mechanical Engineering, York University, Toronto, Canada
*alex.czekanski@lassonde.yorku.ca

Abstract— Thermoplastic polyurethane (TPU) is typically modeled as an isotropic hyperelastic material. However, when fabricated using fused deposition modeling (FDM), it exhibits anisotropic behavior due to directional filament alignment. This study investigates the effects of raster orientation and layer height on the mechanical performance of 3D-printed TPU using uniaxial and planar tensile tests. Four raster angles (0°, 90°, 0/90°, and -45/45°) were tested under uniaxial loading, while planar tests used 0° and 90° orientations. The 0° raster, aligned with the loading direction, showed the highest tensile strength (~9.5 MPa), modulus (~22.85 MPa), and elongation (>250%). The 90° raster displayed the lowest performance, with early failure (~90–100% strain), lower strength (~4–8 MPa), and reduced stiffness (~19.34 MPa), due to weak interlayer bonding. Bidirectional raster angle showed intermediate responses. Planar tensile results confirmed this anisotropy, with 0° specimens reaching ~20 MPa and 230% strain, while 90° specimens failed at ~5 MPa and ~50–60% strain. Microscopy images revealed that reducing layer height from 0.24 mm to 0.18 mm improved interlayer bonding but narrowed raster-to-raster bond widths. These results highlight the strong influence of printing parameters on TPU anisotropy and the need for constitutive models that account for directional effects in 3D-printed soft materials.

Keywords-component; 3D Printing; Elastomers; Anisotropic Behavior; Raster Angles; Hyperelasticity

I. INTRODUCTION

Additive manufacturing (AM) has seen a dramatic rise in research and applications due to its capability to efficiently and precisely fabricate complex structures [1]. Among various AM techniques, Fused Filament Fabrication (FFF) is widely utilized for 3D printing, where a thermoplastic filament is melted and extruded through a nozzle. The molten material is then deposited layer by layer onto a build platform to construct the final part.

Elastomers, a class of soft materials, are extensively employed in engineering applications owing to their unique properties, including high elasticity, energy return, and high damping capacity [2]. These characteristics make them well-suited for demanding applications in the aerospace and automotive industries, such as engine supports, sealing valves, and insulating cables, as well as in additive manufacturing, including the 3D printing of soft robots and soft robotic grippers [3]. Despite the growing adoption of AM, research on the additive manufacturing of elastomers remains relatively limited compared to other materials [4].

Thermoplastic elastomers, such as thermoplastic polyurethanes (TPU), are particularly attractive for 3D printing due to their excellent flexibility, energy return, and shape recovery upon load removal, with minimal permanent deformation. One major challenge in printing soft polymers like TPU is their low stiffness, which prevents processing with some of the standard filament feed extrusion mechanisms, necessitating the use of a direct drive extruder [5]. Additionally, Moisture absorption in TPU significantly impacts the quality and mechanical properties of 3D-printed parts. Research has shown that under-extrusion issues in FFF can occur due to TPU's hygroscopic nature, leading to print failures and variations in tensile strength. Proper filament drying and storage are crucial to mitigating these effects and ensuring consistent extrusion performance [6].

The mechanical properties of 3D-printed soft parts are largely governed by their mesostructure, which is influenced by the process parameters during fabrication of the part. Critical parameters such as void shape, density, fraction, and interlayer bonding significantly impact on the overall mechanical performance of the printed structures [4]. A comprehensive understanding of the effects of process parameters on the hyperelastic behavior of 3D-printed soft materials, particularly under different loading conditions such as tension, compression, and shear, is crucial for expanding their practical applications across various fields [7].

Numerous studies have examined the impact of process parameters on the mechanical behavior of 3D-printed TPU. For instance, Chaudhry and Czekanski analyzed the effects of layer height, infill density, and bidirectional raster orientation on the mechanical properties of TPU specimens under quasi-static uniaxial tensile testing [7]. Similarly, Hohimer et al. investigated the influence of printing parameters such as air gap, raster orientation, and nozzle temperature on ultimate tensile strength (UTS) and material isotropy. Their findings revealed that TPU specimens printed with a negative air gap exhibited nearly isotropic properties, regardless of nozzle temperature and raster orientation [8].

Previous studies in the literature have relied on isotropic hyperelastic models to describe the behavior of 3D-printed TPU parts. However, these models do not fully capture the anisotropic behavior [9-12]. Understanding the anisotropy of 3D-printed soft materials under different loading conditions is essential for selecting an appropriate anisotropic hyperelastic constitutive model that accurately describes their mechanical behavior [13]. To achieve this, the parameters of these models must be identified through curve-fitting approaches using optimization methods that minimize the error between predicted and experimental stress values. A well-formulated constitutive model should accurately describe the nonlinear stress-strain relationship and account for different states of deformation, including uniaxial and planar tensile tests [13].

In this context, this study investigates the effects of raster angles on the anisotropy of 3D-printed parts through uniaxial and planar tension tests. By conducting experiments using a quasi-static testing machine at a low testing rate, this research aims to provide deeper insights into how raster orientation influences the hyperelastic behavior of 3D-printed parts, ultimately contributing to more accurate material modeling and improved design strategies.

II. Materials and Methods

A. Materials and specimens

A TPU filament known as Filaflex 82A, with a hardness of 95 Shore A, was supplied by the company Recreus (Spain). Fabrication of test coupons was performed on a Prusa MK4S printer (filament diameter of 1.75 mm and nozzle diameter of 0.4mm). All test specimens were printed both flat and vertically (up-down) on the build platform. The process parameters were based on the manufacturer's recommendations. Table I summarizes the 3D printing process parameters used to fabricate the uniaxial and planar tensile test samples.

The dimensions of the uniaxial tensile test samples are according to the standard dimensions specified in ASTM D412 and ISO 37 (see Fig. 1). The Plates of $140\ mm \times 100\ mm \times 2\ mm$ were 3D printed with different raster angles: unidirectional (0° and 90°) and bidirectional (0/90° and -45/45°), and were subsequently stamped to produce tensile test samples, as shown in Fig. 2. This approach enabled a smooth and uniform cross-section transition while maintaining both unidirectional and bidirectional orientations without the need for contour line. Additionally, it ensured uniformity across all specimens by minimizing variations caused by edge inconsistencies or defects typically associated with the direct printing of individual samples.

The planar test coupons were 3D printed from a plate measuring 165 mm × 100 mm × 2 mm, with two specimens printed at a time. Two raster angles were considered: unidirectional 0° and 90°, which are sufficient to demonstrate the effects of raster orientation on the anisotropic behavior under pure shear loading conditions.

TABLE I. The 3D Printing Process Parameters

Parameters	Value	Parameters	Value
Nozzle diameter	0.4 mm	Extrusion temperature	$250^o\ C$
Layer height	0.3, 0.24, and 0.18 mm	Bed temperature	$40^o\ C$
Perimeter shells	0	Printing speed	$50\ mm/s$
Infill density	100 %	Closed chamber	Yes

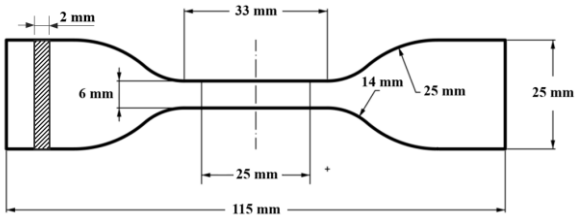

Figure 1. Uniaxial tensile test specimen with dimensions.

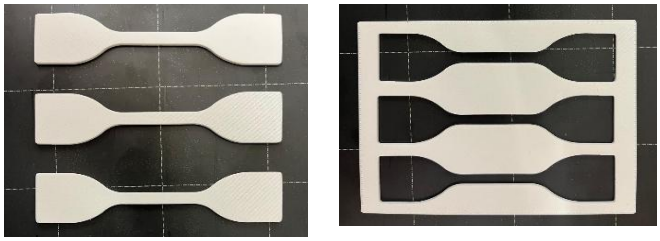

Figure 2. Uniaxial tensile test samples: (a) Stamped specimens and (b) corresponding plate.

B. Mechanical Testing

Uniaxial tensile and planar tensile tests were conducted using an MTS testing machine at ambient temperature (see Fig. 3). A 500 N load cell was used for the uniaxial tensile test, performed according to ASTM D412 Type C and ISO 37 standards, while a 10 kN load cell was used for the planar test. The testing rate was set to 0.1 mm/s for all specimens to analyze the effect of the raster pattern on hyperelastic behavior without being influenced by viscous effects or strain rate dependency. Strain measurements were taken from a 5 mm central region of each specimen using a laser extensometer with a 100 mm capacity.

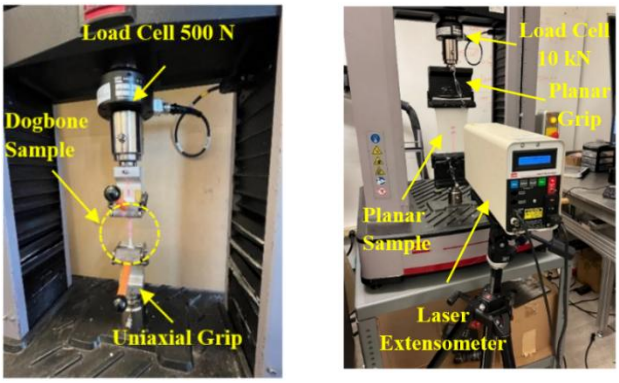

(a) (b)

Figure 3. Experimental setup for (a) uniaxial and (b) planar tensile tests.

III. RESULTS

A. *Uniaxial Tensile Test*

The stress-strain curves in Fig. 4 illustrate the uniaxial tensile behavior of 3D-printed TPU specimens with different raster orientations: 0°, 90°, 0/90°, and -45/45°. All raster orientations exhibit non-linear deformation characteristics, with noticeable variations in mechanical response due to filament alignment. As shown, the 0° raster orientation demonstrates the highest tensile strength and ductility, with stress values reaching approximately 9.5 MPa at 270% strain, owing to optimal filament alignment in the loading direction. The 90° orientation, on the other hand, exhibits the lowest strength and stiffness, with stress values peaking around ~8 MPa at the same strain level. This reduced performance is attributed to the raster being perpendicular to the loading axis, resulting in weaker interlayer bonding and an increased risk of delamination. The bidirectional raster orientations (-45/45° and 0/90°) show intermediate mechanical responses.

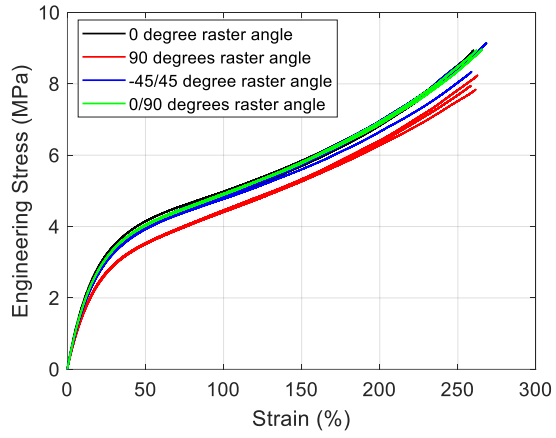

Figure 4. Stress-strain curves for 3D-printed samples with different raster angles and 0.3mm layer height.

Fig. 5 illustrates the calculated Young's modulus for samples printed with raster angles of 0°, 90°, 0/90°, and -45/45°, based on three test repetitions. The modulus values were determined from the slope of the regression line fitted to the initial linear-elastic region of the stress-strain curves (axial strain below 5% strain (0.05 mm/mm)). The results reveal that the 0° raster angle exhibited the highest average modulus of 22.85 MPa, while the 90° raster angle showed the lowest average modulus at 19.34 MPa, likely due to weaker interlayer bonding. The ±45° and 0/90° configurations yielded intermediate moduli of 21.41 MPa and 21.78 MPa, respectively, suggesting balanced mechanical performance between stiffness and flexibility.

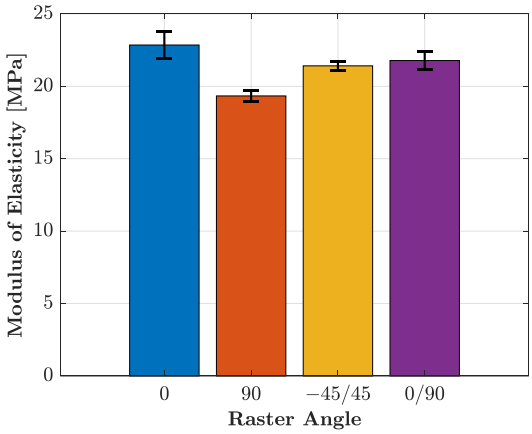

Figure 5. Comparison of modulus of elasticity for different raster angles and 0.3mm layer height.

B. *Effect of Layer Height*

The stress-strain curves for 3D-printed TPU specimens with 0° and 90° raster angles under uniaxial tensile loading is shown in Fig. 6. The black curves represent the 0° raster orientation, while the red curves correspond to the 90° raster orientation. The 0° orientation exhibits a significantly higher tensile strength and elongation, with stress values approaching 9 MPa and strain exceeding 250%, indicating superior load-bearing capacity due to filament alignment in the loading direction. In contrast, the 90° orientation displays lower tensile strength (~4 MPa) and early failure around 90–100% strain, attributed to weak interlayer bonding and filament alignment perpendicular to the loading axis.

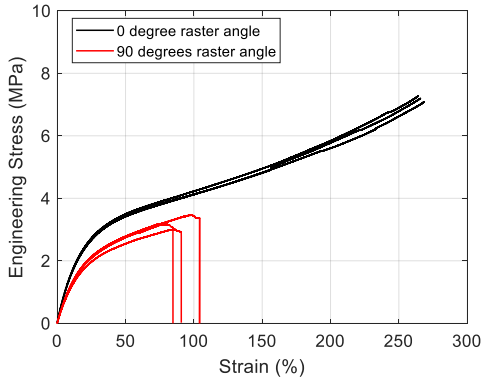

Figure 6. Stress-strain response of 3D-printed TPU specimens with 0° and 90° raster angles and 0.18mm layer height.

C. Microscope Results

The influence of layer height on the mesostructure and bonding characteristics of the printed specimens is presented in Figs 6 and 7. Figure 6 visually compares the cross-sectional mesostructure for two different layer heights (0.24 mm and 0.18 mm), highlighting noticeable differences in the raster-to-raster and interlayer bond widths. Quantitative results, summarized in Fig. 7, indicate that reducing the layer height from 0.24 mm to 0.18 mm significantly increased the interlayer bond width, suggesting improved vertical bonding between successive layers. Conversely, reducing the layer height (0.18 mm) resulted in a narrower raster-to-raster bond width compared to the higher layer height (0.24 mm), indicating enhanced horizontal bonding at increased layer heights.

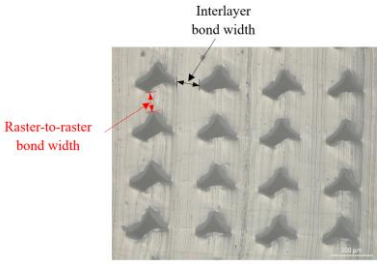

(a) 0.24 mm

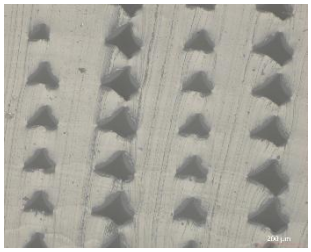

(b) 0.18 mm

Figure 7. Effects of layer height on the mesostructure of the printed parts.

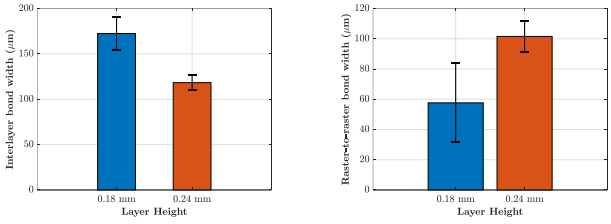

(a) (b)

Figure 8. Effect of layer height on the (a) interlayer bond width and (b) raster-to-raster bond width.

D. Planar Tensile Test (Pure Shear)

The stress-strain responses of 3D-printed TPU under planar (pure shear) loading conditions exhibit significant anisotropy, as shown in Fig. 7. The specimens printed with a 0° raster angle (aligned with the loading direction) exhibited higher ultimate tensile strength (~20 MPa) and greater large deformation, with failure occurring at approximately 230% strain. This behavior is attributed to the continuous filament alignment along the loading axis, which enhances load-bearing capacity.

Conversely, the 90° raster angle specimens (perpendicular to the loading direction) exhibited significantly lower mechanical properties, failing at a strain of ~50–60% and a maximum stress of ~5 MPa. This reduction in strength and strain capacity results from interlayer adhesion being the primary load-bearing mechanism, which is inherently weaker than the filament material itself.

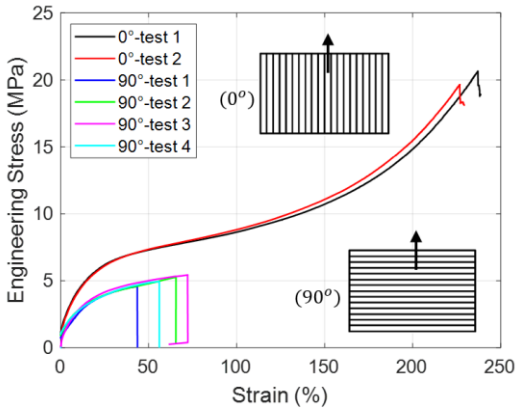

Figure 9. Stress-strain curves for 3D-printed samples with different raster angles (0° and 90°) and 0.3mm layer height.

IV. Conclusion

This study confirms the significant influence of raster orientation on the mechanical behavior of 3D-printed TPU under uniaxial and planar (pure shear) loading. Specimens with a 0° raster angle, aligned with the loading direction, demonstrated the highest strength and ductility, with no failure observed at large strains and the greatest stiffness due to optimal filament alignment. In contrast, specimens with a 90° raster angle exhibited early failure, reduced strength, and the lowest stiffness, primarily due to weak interlayer bonding. Bidirectional raster configurations (0/90° and -45/45°) showed intermediate performance, balancing strength and flexibility under high deformation. Planar testing further emphasized the anisotropic response. Specimens with a 0° raster orientation outperformed those with a 90° raster, which failed earlier and showed significantly lower strength and strain capacity. These findings highlight the importance of selecting appropriate raster orientations when designing 3D-printed components for load-bearing applications involving large deformation.

The experimental results provide valuable insight for evaluating and calibrating constitutive models that capture the anisotropic and hyperelastic behavior of 3D-printed soft materials. Accounting for directional effects is crucial for accurate simulation and for expanding the use of 3D-printed elastomers across various advanced applications.

Acknowledgment

All authors acknowledge the support of the Lassonde School of Engineering at York University. This research was funded by the Natural Sciences and Engineering Research Council of Canada (NSERC SMART-ART CREATE 555425-2021) as well as the Canadian Space Agency (CSA FAST 2024).

References

[1] Y. Wang, T. Wu, and G. Huang, “State-of-the-art research progress and challenge of the printing techniques, potential applications for advanced ceramic materials 3D printing,” Aug. 01, 2024, Elsevier Ltd. doi: 10.1016/j.mtcomm.2024.110001.

[2] I. M. Alarifi, “A comprehensive review on advancements of elastomers for engineering applications,” Oct. 01, 2023, KeAi Communications Co. doi: 10.1016/j.aiepr.2023.05.001.

[3] Y. A. AboZaid, M. T. Aboelrayat, I. S. Fahim, and A. G. Radwan, “Soft robotic grippers: A review on technologies, materials, and applications,” Jul. 01, 2024, Elsevier B.V. doi: 10.1016/j.sna.2024.115380.

[4] V. M. Bruère, A. Lion, J. Holtmannspötter, and M. Johlitz, “The influence of printing parameters on the mechanical properties of 3D printed TPU-based elastomers,” Progress in Additive Manufacturing, vol. 8, no. 4, pp. 693–701, Aug. 2023, doi: 10.1007/s40964-023-00418-7.

[5] N. Kumar, P. K. Jain, P. Tandon, and P. M. Pandey, “The effect of process parameters on tensile behavior of 3D printed flexible parts of ethylene vinyl acetate (EVA),” J Manuf Process, vol. 35, pp. 317–326, Oct. 2018, doi: 10.1016/j.jmapro.2018.08.013.

[6] V. M. Bruère, A. Lion, J. Holtmannspötter, and M. Johlitz, “Under-extrusion challenges for elastic filaments: the influence of moisture on additive manufacturing,” Progress in Additive Manufacturing, vol. 7, no. 3, pp. 445–452, Jun. 2022, doi: 10.1007/s40964-022-00300-y.

[7] M. S. Chaudhry and A. Czekanski, “Evaluating FDM process parameter sensitive mechanical performance of elastomers at various strain rates of loading,” Materials, vol. 13, no. 14, Jul. 2020, doi: 10.3390/ma13143202.

[8] C. Hohimer, J. Christ, N. Aliheidari, C. Mo, and A. Ameli, “3D printed thermoplastic polyurethane with isotropic material properties,” in Behavior and Mechanics of Multifunctional Materials and Composites 2017, SPIE, Apr. 2017, p. 1016511. doi: 10.1117/12.2259810.

[9] M. Zahed, R. Ardeshiri Joungheghani, and M. Safarabadi, “Reinforcement of 3D-Printed Re-Entrant Structures using Additional Supports under Three-Point Bending, Experimental and Numerical Analyses,” *Adv Eng Mater*, vol. 26, no. 1, Jan. 2024, doi: 10.1002/adem.202301252.

[10] Herianto, W. Irawan, A. S. Ritonga, and A. Prastowo, “Design and fabrication in the loop of soft pneumatic actuators using fused deposition modelling,” *Sens Actuators A Phys*, vol. 298, Oct. 2019, doi: 10.1016/j.sna.2019.111556.

[11] E. Gasparotti *et al.*, “A 3D printed melt-compounded antibiotic loaded thermoplastic polyurethane heart valve ring design: an integrated framework of experimental material tests and numerical simulations,” *International Journal of Polymeric Materials and Polymeric Biomaterials*, vol. 68, no. 1–3, pp. 1–10, Feb. 2019, doi: 10.1080/00914037.2018.1525717.

[12] C. H. Liu, Y. Chen, and S. Y. Yang, “Quantification of hyperelastic material parameters for a 3D-Printed thermoplastic elastomer with different infill percentages,” *Mater Today Commun*, vol. 26, Mar. 2021, doi: 10.1016/j.mtcomm.2020.101895.

[13] Jörgen Bergström, *Mechanics of Solid Polymers Theory and Computational Modeling*. William Andrew, imprint of Elsevier, 2015.